Electronic Supplementary Information

Near-infrared aggregation-induced emission nanodots for early diagnosis of tongue squamous cell carcinoma and sentinel lymph nodes mapping

Guan-Meng Zhang,[a,#] Di Jiao,[b,#] Shao-Chen Nie,[c] Zhao-Yuan Xu,[a] Xiaoyan Zhang,[a] Yanmei Dai,[a,d] Mai-Ning Jiao,[c] Hanlin Ou,*[,b] Ying-Bin Yan,*[,a,d] Dan Ding*[,a,b,d]

[a.] Department of Oromaxillofacial-Head and Neck Surgery, Tianjin Stomatological Hospital, and Hospital of Stomatology, Nankai University, Tianjin 300041, China.

[b.] State Key Laboratory of Medicinal Chemical Biology, Key Laboratory of Bioactive Materials, Ministry of Education, and College of Life Sciences, Nankai University, Tianjin 300071, China

[c.] Tianjin Medical University, Tianjin 300070, China.

[d.] Tianjin Key Laboratory of Oral and Maxillofacial Function Reconstruction, Tianjin Stomatological Hospital, and Hospital of Stomatology, Nankai University, Tianjin 300041, China.

#These authors contributed equally to this work.

*Correspondence should be addressed to H. O. (hlou@nankai.edu.cn), Y. Y. (yingbinyan@qq.com), and D. D. (dingd@nankai.edu.cn).

Table of Contents

Experimental Procedures

Materials. All chemicals were obtained from Sigma-Aldrich unless otherwise specified and used as received without further purification. 1,2-Distearoyl-sn-glycero- 3-phosphoethanolamine-N-[methoxy(polyethylene glycol)-2000] (DSPE-PEG2000; Lipid-PEG2000) was purchased from Laysan Bio, Inc. (Arab, AL). The solvents for chemical reactions were distilled before use. Compounds DPA-TPE-Br and Ph-DCM were synthesized according to the literature[1].

Characterization. ^{1}H and ^{13}C nuclear magnetic resonance (NMR) spectra were recorded on a Bruker-DPX 400 spectrometer. Chemical shifts are reported in ppm from tetramethylsilane with solvent resonance as the internal standard. High-resolution mass spectra (HRMS) were recorded on a Varian 7.0T FTMS mass spectrometer system operating in matrix-assisted laser desorption/ionization time of flight (MALDI-TOF) mode. UV–vis absorption spectra were recorded on a Shimadzu UV-1700 spectrometer. Photoluminescence and afterglow spectra were recorded on a Perkin-Elmer LS 55 spectrofluorometer. The observation of nanoparticle morphology was investigated using transmission electron microscopy (TEM, JEM-2010FJEOL, Japan). Size distribution of nanoparticles was conducted on dynamic light scattering (DLS) with a particle size analyzer (90 Plus, Brookhaven Instruments Co. USA) at a fixed angle of 90° at room temperature. Afterglow images and NIR fluorescent images were acquired using the Xenogen IVIS® Lumina II system under bioluminescence and fluorescence modes, respectively. Structures of DPA-TPE-DCM were obtained using the Gaussian 09 W program at the B3LYP/6-31G(d) level, Gaussian 09 program.

Synthesis and characterization of DPA-TPE-aldehyde. DPA-TPE-Br was first synthesized according to the literature[1]. Under argon atmosphere， 2.4 M n-BuLi (1.5 equiv) was added dropwise to a stirred solution of DPA-TPE-Br (1.0 equiv) in dry THF at -78 °C. The mixture was stirred at -78°C for 4 h and dry DMF (3.0 equiv) was added rapidly. The reaction was then continued at room temperature with stirring for 6 h before adding saturated aqueous ammonium chloride solution to quench the reaction and extracting to collect the organic phase. The organic layer collector was rinsed with brine and then treated with anhydrous Na_2SO_4 and evaporated to dryness under reduced pressure.. Purify the crude product by

column chromatography to give DPA-TPE-CHO (yield 41%). ^{1}H NMR (400 MHz, DMSO) δ 9.88 (s, 1H), 7.66 (d, J = 6.7 Hz, 2H), 7.28 (t, J = 6.9 Hz, 4H), 7.23 – 7.11 (m, 8H), 7.06 – 6.97 (m, 6H), 6.94 (d, J = 7.6 Hz, 4H), 6.86 (d, J = 6.8 Hz, 2H), 6.72 (d, J = 6.8 Hz, 2H).

Synthesis and characterization of DPA-TPE-DCM. Ph-DCM was first synthesized based on the literature report[2]. Under an argon atmosphere, piperidine (0.1 equiv) was added to a stirred solution of DPA-TPE-aldehyde (1.0 equiv) and Ph-DCM (1.0 equiv) in dry acetonitrile. The reaction solution was stirred and refluxed under heating at 80°C for 12 hours, and then filtered. The residue was washed with acetonitrile and dried under vacuum to obtain DPA-TPE-DCM (yield 98%) (yield 98%). ^{1}H NMR (400 MHz, $CDCl_3$) δ 8.91 (d, J = 8.1 Hz, 1H), 7.73 (t, J = 7.3 Hz, 1H), 7.53 (d, J = 12.3 Hz, 2H), 7.45 (t, J = 6.6 Hz, 1H), 7.31 (d, J = 5.7 Hz, 2H), 7.19 – 6.96 (m, 21H), 6.88 – 6.64 (m, 7H).

Preparation of DPA-TPE-DCM NPs. DPA-TPE-DCM nanoparticles were prepared by the classical nanoprecipitation method. 1 mg of DPA-TPE-DCM and 4 mg of DSPE-PEG_{2000} were dissolved in 1 mL of THF, and the mixture was slowly dropped into 9 mL of water (sonicated for 3 min) under the action of a microtip probe sonicator (XL2000, Misonix Incorporated, NY). The aqueous solution of DPA-TPE-DCM nanoparticles was obtained by promoting the volatilization of THF using an air pump. Finally, the solution was purified and filtered using a 0.45 μm syringe-driven filter followed by ultrafiltration at 5000 rpm for 10 min.

In vitro optical characterization. To evaluate the molecular AIE properties, fluorescence spectra of TPA-DPE-DCM in tetrahydrofuran/water mixture were measured by fluorescence spectrophotometer. Firstly, DPA-TPE-DCM (1.4 mg) was dissolved in THF (1 mL), and the absorption spectrum of this solution was measured by UV-Vis. Subsequently, the emission spectra (λex=451 nm) of TPA-DPE-DCM in different ratios of THF/water mixture (1 μM, 3 mL) were measured at the maximum absorption using a fluorescence spectrophotometer. To measure the fluorescence quantum yield of TPA-DPE-DCM NPs, ICG was used as a standard substance with a known fluorescence quantum yield (Φ) value of 2.5% in H_2O. The fluorescence quantum yield (Φ) was calculated according to the following equation[2]:

$$\Phi_{sample} = \Phi_{standard} \times (A_{sample}/A_{standard}) \times (Abs_{standard}/Abs_{sample}) \times (\eta_{standard}/\eta_{sample})^2$$

In vitro cytotoxicity study. To evaluate the cytotoxicity of the synthesized probe, Cell Counting Kit-8 (CCK-8) assays were used to detect the effect of the DPA-TPE-DCM NPs on cell activity against both cancer and normal cells. Mouse squamous cell carcinoma cells 7 (SCC7) and human periodontal ligament fibroblasts (HPDLFs) were seeded into a 96-well plate at a cell density of 5000 cells per well for 24 h. Then, the cells were treated with DPA-TPE-DCM NPs at different concentrations (0, 3.125, 6.25, 12.5, 25 and 50 μg/mL) and coincubated for another 24 h in the dark. After that, the original culture medium was discarded, and 110 μL of freshly prepared CCK-8 solution in culture medium (1:10) was added to each well. After an additional 2 h incubation in the incubator, the absorbance of the suspension was recorded by a microplate reader at a wavelength of 450 nm, and the relative cell viability was calculated by the following equation:

$$\text{cell viability (\%)} = (OD_{sample} - OD_{background})/(OD_{control} - OD_{background}) \times 100\%.$$

Hemolytic test. Fresh blood was collected from SD rats, and red blood cells (RBCs) were retained after repeated washing and centrifugation with normal saline 3 times. Various concentrations (12.5, 25, 50, 100, 200 μg/mL) of DPA-TPE-DCM NPs were coincubated with RBCs for 1 h, 2 h and 3 h at 37 ℃. RBCs were incubated with double-distilled water as the positive control for hemolysis, while normal saline was used as the negative control. The incubated solution was photographed every 1 h, and a blood smear was taken to observe the morphological changes of red blood cells. Three hours later, the absorbance of the supernatant at 540 nm was recorded by a microplate reader, and the hemolysis ratio (HR) was calculated following the formula:

$$HR\ (\%) = (OD_{sample}-OD_{negative\ control})/\ (OD_{positive}-OD_{negative\ control}) \times 100\%$$

In vivo toxicity study. Healthy C3H mice were randomly divided into two groups: group I: control group, and group II: DPA-TPE-DCM nanoparticles (6 mice in each group). On day 0, mice in group I were intravenously injected with 200 μL of normal saline; mice in group II were intravenously injected with 200 μL of DPA-TPE-DCM nanoparticles (concentration: 1 mg/mL). The body weight changes across the experiment were recorded. Two weeks later,

two groups of mice were sacrificed to collect the main organs, including the heart, liver, spleen, lung and kidney, for pathological examination. The histological sections were stained with hematoxylin and eosin (H&E) and imaged under an optical microscope.

Biodistribution study

The biodistribution of the DPA-TPE-DCM NPswas studied. Tumor-bearing C3H mice were injected with 200 μL DPA-TPE-DCM NPs through the tail vein. Twelve hours later, the mice were sacrificed, and their major organs (heart, liver, spleen, lung and kidney) were excised and imaged by an IVIS Spectrum imaging system (excitation filter 465, emission filter Cy5.5).

The Cell Image of DPA-TPE-DCM NPs

After verifying the biosafety of DPA-TPE-DCM NPs, an in vitro cell imaging study was carried out. SCC7 cells were incubated in confocal imaging chambers with DPA-TPE-DCM NPs in culture medium at a concentration of 0.1 mg/mL for 12 hours at 37 ℃ in a humidified atmosphere of 5% CO_2. The cells were washed with phosphate buffered solution (PBS) three times to remove the fluorescent probes that were not absorbed by the cells and then fixed with 4% paraformaldehyde for 15 min. Subsequently, intracellular fluorescence images were captured by confocal laser scanning microscopy (CLSM) to determine the potential of DPA-TPE-DCM NPs as a biological imaging dye after staining with 2-(4-Amidinophenyl)-6-indolecarbamidine dihydrochloride (DAPI) for 10 min. The imaging of SCC7 cells was captured by CLSM under excitation light sources of 405 nm (DAPI) and 488 nm (DPA-TPE-DCM NPs).

Cell line origin and identification. The human periodontal ligament fibroblasts (HPDLFs) used for the experiment were obtained from a patient, 25-year-old, in the the alveolar surgery clinic of Tianjin Stomatological Hospital. The patient signed an informed consent form and agreed to allow us to use his tissue in our research work. HPDLFs were obtained from the roots of extracted impacted human maxillary third molar teeth. Immediately after extraction, the teeth were placed in Dulbecco's Modified Eagle's Medium

(DMEM) at 4 °C. The teeth were washed repeatedly with PBS containing 100 U/mL penicillin and 100 μg/mL streptomycin. Periodontal ligament tissues attached to the middle third of the roots were gently curetted off and placed in DMEM containing 20% FBS and 1% penicillin/streptomycin solution. These tissues were minced and rinsed in DMEM, then allowed to attach to the bottom of tissue culture flasks. DMEM supplemented with 20% FBS and antibiotics were added to the flasks followed by incubation at 37 °C and 5% CO_2 until fibroblast-like cells had grown to confluency. After 2 to 3 weeks of culture, cells from the second to fourth passages were harvested for later experiments.

The SCC7 cell line was kindly received from Prof. Yixiang Wang, School of Stomatology, Peking University. In the clinicopathological diagnosis of tumors, in addition to H&E staining techniques, immunohistochemical tests can also be used to assist in the diagnosis. Oral squamous cell carcinoma (OSCC) comes from epidermisinoral cavity and most of them develop from precancerous lesion of oral mucousmembrane. Commonly used immunohistochemical markers are squamous epithelial cell markers: AE1/AE3 (CK pan), CKHMW, CK5/6 and p63. Cytoeratin (CK) is expressed in pairs in the cytoplasm of epithelial cells as a characteristic marker of epithelial cells. P63 can be used as a marker of squamous carcinoma and is expressed in the nucleus of squamous carcinoma cells. In contrast, vimentins are expressed in the cytoplasm of mesenchymal cells, which can be used as a control group[3, 4].

The biological characteristics of oral squamous carcinoma cells can be reflected by cell morphology. Observation of cell morphology: under the microscope, they were polygonal and evenly distributed like paving stones. Immunohistochemical staining: P63 stained positive in the nuclei of SCCs. Keratin stained positive in the cytoplasm of OSCCs. No positive staining was found in OSCCs of Vimentin control group. Subsequently, in vivo tumorigenesis experiment was conducted to observe the tumorigenesis situation. Histopathological changes were observed by H&E staining of the tumor tissue. Therefore, this cell line could be considered as squamous cell carcinoma.

Establishment of an animal model of tongue squamous cell carcinoma

Animal models are the basis of the diagnosis and treatment of oral squamous cell carcinoma. SCC7 used in this study is an established cell line from OSCC in the oral floor of mice and grows without being affected by the immune system. In this study, this cell line was first used to develop an animal model of tongue squamous cell carcinoma[5-7]. This model can reflect the clinical characteristics of tumors and is an effective and useful method to elucidate the mechanism of tumor invasion and treatment. Cell culture: SCC7 cells were cultured in DMEM supplemented with 10% fetal bovine serum (FBS), 100 units/mL penicillin and 100 mg/mL streptomycin at 37 °C in a humidified atmosphere of 5% CO_2. In the fourth generation, when the cells covered the bottom of the bottle to more than 80% (Figure S), dissociation and counting of SCC7 cells at the logarithmic growth phase were conducted, and PBS was added to make a cell suspension (adjust the cell density to 3×10^7/mL). Method: The experimental animals consisted of twelve male C3H mice (mouse weight ~20 g). They were equally divided into two groups: the control group and the SCC7 transplanted group. In the SCC7-transplanted group, the SCC7 cell suspension was injected into the tongue of mice with a 1 mL syringe and No. 6 needle, and an 80 μl cell suspension was injected into each mouse. Meanwhile, the same amount of PBS was injected into the tongue of mice of the control group in the same way. After that, the mice were put back into the cage, and the feeding method was the same as before.

DPA-TPE-DCM NPs for in vivo fluorescence tumor diagnosis and image-guided surgery

Next, to evaluate the diagnostic effect of DPA-TPE-DCM on tongue squamous cell carcinoma (TSCC), in vivo fluorescence imaging of the AIE probe was performed on tumor-bearing mice by an IVIS Spectrum imaging system (excitation wavelength 465 nm, emission filter Cy5.5). DPA-TPE-DCM NPs (200 μL, 1 mg/mL based on DPA-TPE-DCM) were injected into mice via the tail vein in advance. Twelve hours after injection, the probe entered the tumor tissue through the blood circulation according to the EPR effect. Then, the mice were anesthetized, and in vivo imaging was performed by the IVIS Spectrum imaging system. The signal-to-background (S/B) ratio is calculated as S/B ratio = (S_{tumor} - S_{board})/($S_{nomal\ tissue}$ -

S_{board}), where S_{tumor}, $S_{nomal\ tissue}$, and S_{board} are the signal intensity of tumor, adjacent tissue, and board obtained at imaging, respectively. Under the image instructions, the tumor tissues were excised and fixed in 4% paraformaldehyde overnight. Then, the samples were embedded in paraffin, sectioned, and stained with hematoxylin and eosin (H&E) to determine the nature of the tissue obtained.

In vivo fluorescence imaging of the SLN

DPA-TPE-DCM NPs (50 μL) were injected into the tongue of tumor-bearing mice in advance. The lymphatic system of mice was imaged at 8 h postinjection. After carefully dissecting the superficial skin, the lymph nodes were excised out and pathologically examined.

Animal ethics

All animal experiments were performed in duly in compliance with the guidelines set by the Tianjin Committee of Use and Care of Laboratory Animals, and the overall project protocols were approved by the Animal Ethics Committee of Institute of Radiation Medicine, Chinese Academy of Medical Sciences. All mice were obtained from the Laboratory Animal Center of the Institute of Radiation Medicine, Chinese Academy of Medical Sciences.

Supplementary figures

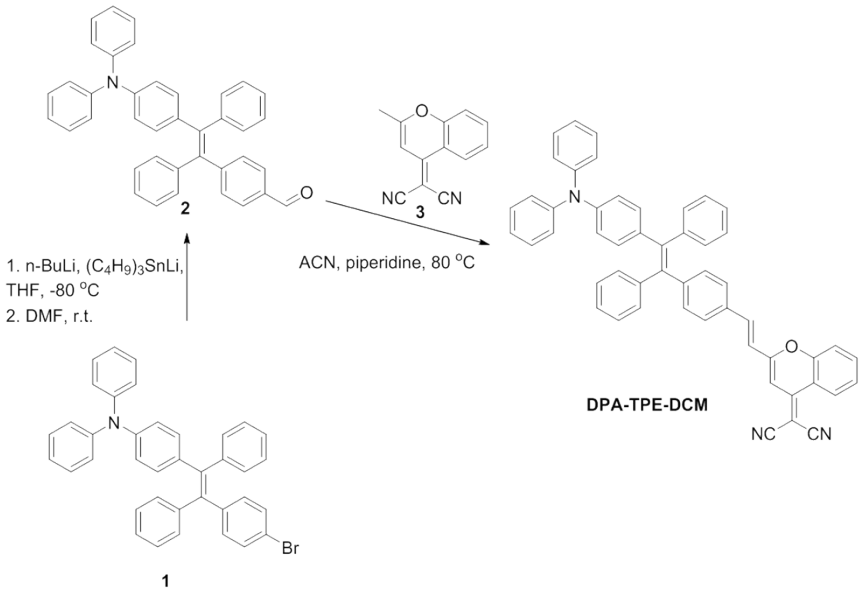

Figure S1. Synthetic route of DPA-TPE-DCM.

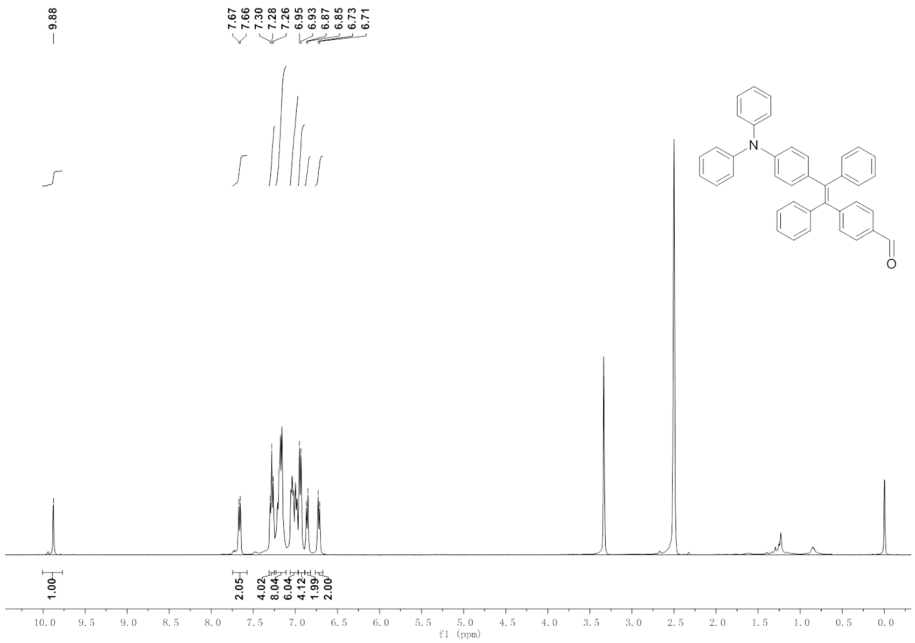

Figure S2. ^{1}H NMR spectrum of DPA-TPE-aldehyde in DMSO.

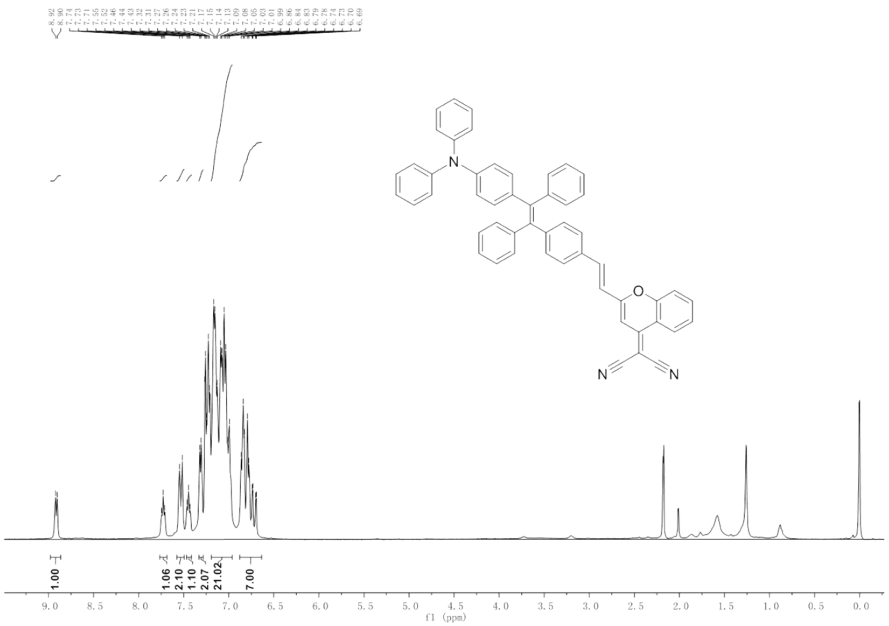

Figure S3. ^{1}H NMR spectrum of DPA-TPE-DCM in $CDCl_3$.

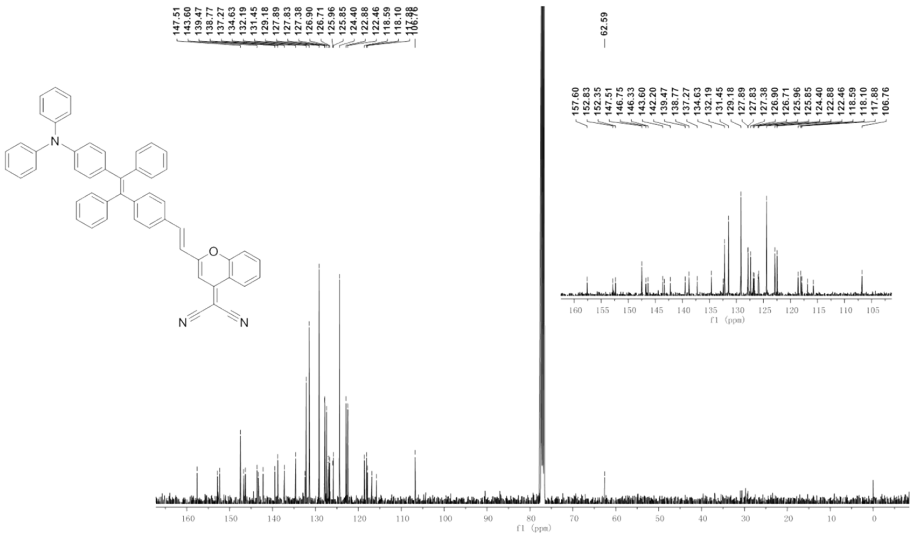

Figure S4. ^{13}C NMR spectrum of DPA-TPE-DCM in $CDCl_3$.

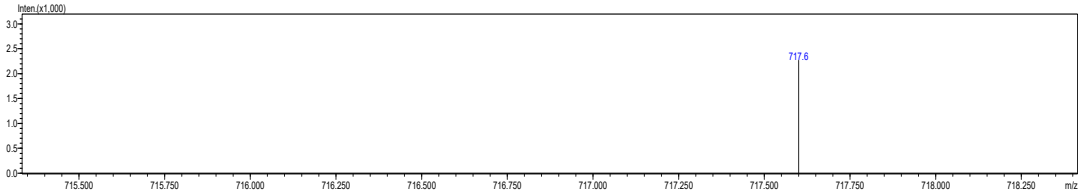

Figure S5. Mass spectrum of DPA-TPE-DCM.

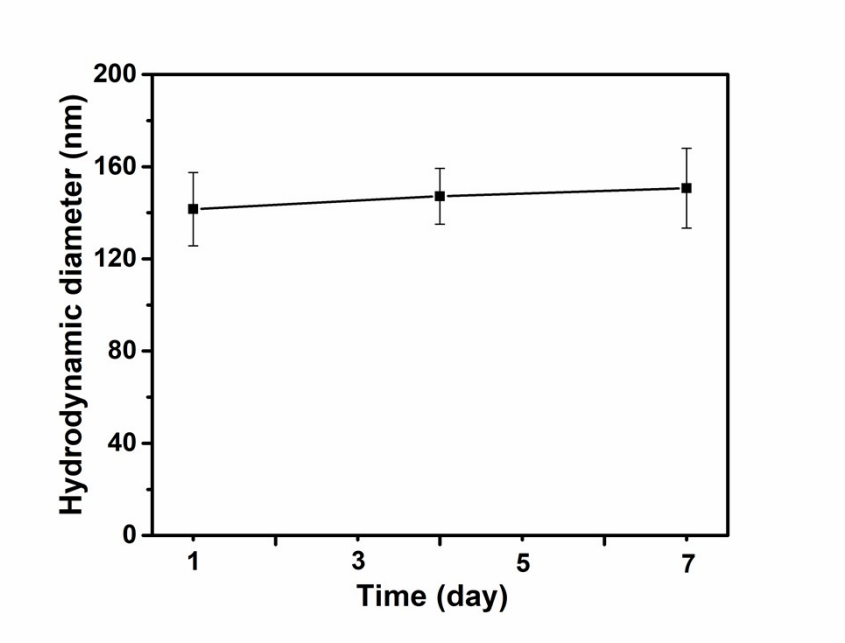

Figure S6. Colloidal stability of DPA-TPE-DCM NPs in water with time.

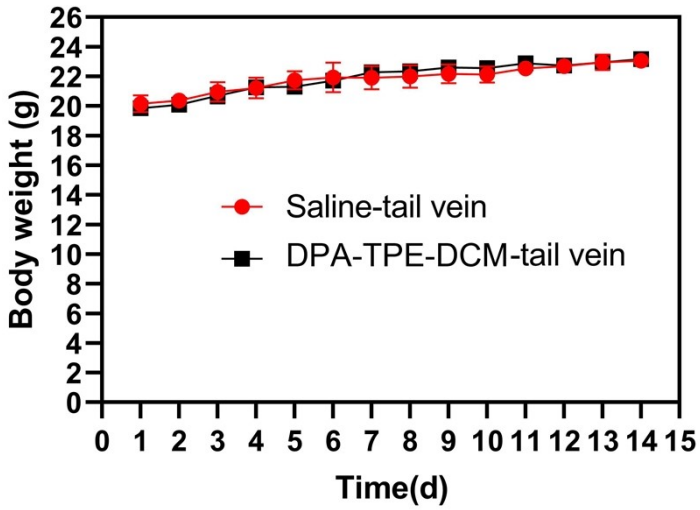

Figure S7. Body weight changes of mice with intravenous injection of DPA-TPE-DCM NPs and saline (n = 6 per group), respectively.

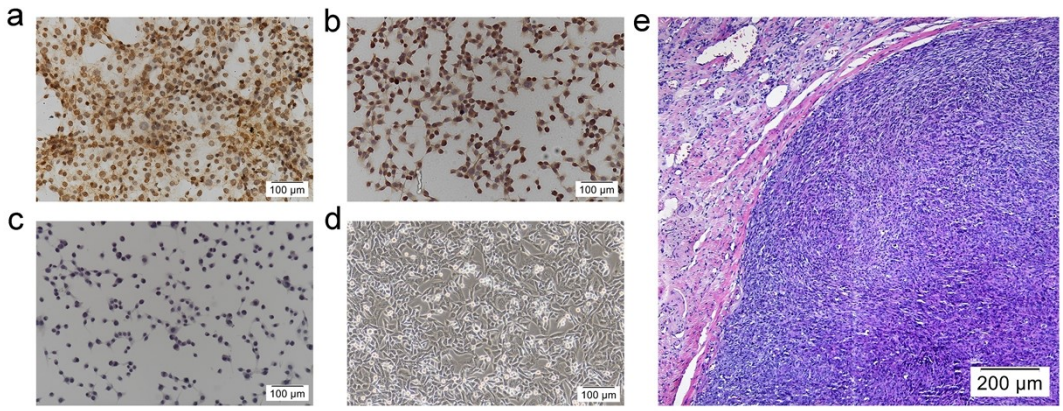

Figure S8. Immunocytochemistry stained images of P63 (a), CK pan (b) and vimentin (c) of SCC7. (d) Bright field image of SCC7. (e) H&E histological analyses for the obtained tumor tissue.

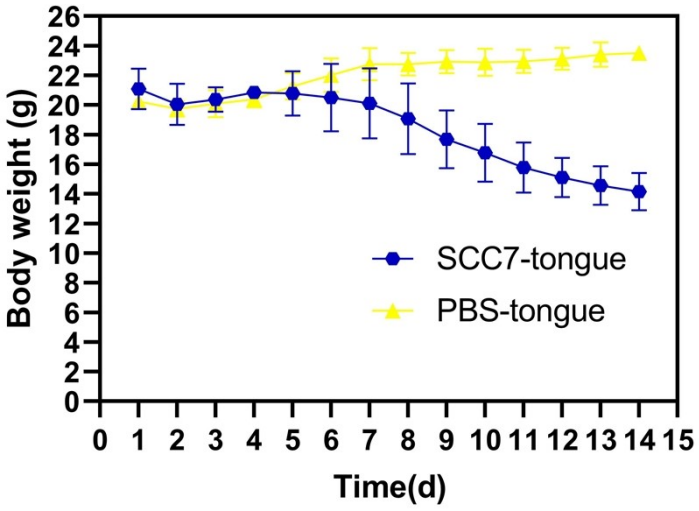

Figure S9. Body weight changes of mice with tongue injection of SCC7 and PBS buffer (n = 6 per group).

Table S1. Summary of signal-to-background (S/B) ratios for the recently reported fluorescent agents with similar emission wavelengths to DPA-TPE-DCM NPs.

Fluorescent agents	Excitation wavelength (nm)	Maximum emission wavelength (nm)	Targeted tissue or disease	S/B Ratio	Reference
Ir-Im-PEG	595	705	Hepatic H22 tumours	10	[8]
a-DTPEBBTD-C4	635	780-820	Abdominal carcinoma	7.2	[9]

ICG/MSNs-RGD	780	840	Liver Cancer	6.0 ± 0.8	[10]
ICG	778	830	Pulmonary Nodules	1.5–4.4 (mean 2.2)	[11]
ICG-Glu-Glu-AE105	745	-	Tongue tumor	2.5	[12]

Reference

1. L. Chen, Y. Jiang, H. Nie, R. Hu, H. S. Kwok, F. Huang, A. Qin, Z. Zhao and B. Z. Tang, *ACS Applied Materials & Interfaces*, 2014, **6**, 17215-17225.
2. A. T. R. Williams, S. A. Winfield and J. N. Miller, *Analyst*, 1983, **108**, 1067-1071.
3. P. G. Chu and L. M. Weiss, *Histopathology*, 2002, **40**, 403-439.
4. T. R. Helliwell and T. E. Giles, *The Journal of Laryngology & Otology*, 2016, **130**, S59-S65.
5. B. W. O'Malley, K. A. Cope, S. H. Chen, D. Li, M. R. Schwarta and S. L. Woo, *Cancer Res*, 1996, **56**, 1737-1741.
6. B. W. O'Malley, Jr., K. A. Cope, C. S. Johnson and M. R. Schwartz, *Arch Otolaryngol Head Neck Surg*, 1997, **123**, 20-24.
7. T. Nomura, T. Shibahara, A. Katakura, S. Matsubara and N. Takano, *Oral Oncol*, 2007, **43**, 257-262.
8. X. Zheng, H. Mao, D. Huo, W. Wu, B. Liu and X. Jiang, *Nat Biomed Eng*, 2017, **1**, 0057.
9. J. Liu, C. Chen, S. Ji, Q. Liu, D. Ding, D. Zhao and B. Liu, *Chemical Science*, 2017, **8**, 2782-2789.
10. C. Zeng, W. Shang, K. Wang, C. Chi, X. Jia, C. Fang, D. Yang, J. Ye, C. Fang and J. Tian, *Sci. Rep.*, 2016, **6**, 21959.
11. O. T. Okusanya, D. Holt, D. Heitjan, C. Deshpande, O. Venegas, J. Jiang, R. Judy, E. DeJesus, B. Madajewski, K. Oh, M. Wang, S. M. Albelda, S. Nie and S. Singhal, *The Annals of Thoracic Surgery*, 2014, **98**, 1223-1230.
12. A. Christensen, K. Juhl, M. Persson, B. W. Charabi, J. Mortensen, K. Kiss, G. Lelkaitis, N. Rubek, C. von Buchwald and A. Kjær, *Oncotarget*, 2017, **8**, 15407-15419.